

ASSESSMENT ON THE EFFECTS OF THE OPERATIONAL CONDITIONS ON THE MANUFACTURE OF PLA-BASED COMPOSITES USING AN INTEGRATED COMPOUNDING-INJECTION MOULDING MACHINE

Daniel GONZÁLEZ^{a1,b}, Ana Rita CAMPOS^c, Antonio M. CUNHA^d, Valentín SANTOS^{a2,b,*} and Juan Carlos PARAJÓ^{a3,b}

^a Chemical Engineering Department, Politecnical Building, Campus Ourense, University of Vigo, 32004 Ourense, Spain; e-mail: ¹ danilson@uvigo.es, ² vsantos@uvigo.es, ³ jcparajo@uvigo.es

^b CITI, Investigation, Transfer and Innovation Center, Avda. Galicia No. 2, Parque Tecnolóxico de Galicia, San Cibrao das Viñas, 32900 Ourense, Spain

^c PIEP – Innovation in Polymer Engineering, Campus de Azurém, 4800-058 Guimarães, Portugal; e-mail: r.campos@piep.pt

^d IPC – Institute for Polymers and Composites, Department of Polymer Engineering, University of Minho, Campus de Azurém, 4800-058 Guimarães, Portugal; e-mail: amcunha@dep.uminho.pt

Received August 19, 2011

Accepted October 31, 2011

Published online December 16, 2011

Cellulose fibres were employed as reinforcement agent for biodegradable composites using polylactic acid (PLA) as a polymer matrix. PLA can be obtained from renewable resources, and it is attracting much interest owing to its favourable physico-mechanical properties and biodegradability. Prior to composite compounding, two commercial PLA from different suppliers were characterized for apparent density, flow index, crystallinity, thermal properties, melt flow rheology and intrinsic viscosity for comparison. In experiments performed with an integrated compounding-injection moulding machine (ICIM), the effects of the processing conditions on the mechanical properties of composites (tensile strength, stiffness and strain at break) were analyzed using a Taguchi experimental design. Other properties of the composites, such as surface morphology and fibre length distribution, were also considered. ICIM technology provided composites with better mechanical properties and lower fibre degradation than the conventional sequential extrusion and injection moulding (SEIM) technology.

Keywords: Renewable resources; Materials science; Polymers; Polylactide; Biomass; Biocomposites; Mechanical properties; Injection moulding.

The interest in using environmentally friendly materials is growing due to increasing sustainability concerns and volatile oil prices. In the near future, biobased biodegradable thermoplastic polymers such as polylactic acid (PLA) and polyhydroxyalkanoates (PHA) are expected to replace at least a

part of conventional thermoplastics (such as polypropylene, polyethylene, polystyrene, or polyvinyl chloride)^{1,2}.

Polylactic acid (PLA) was one of the first biobased plastic produced at a large scale (Natureworks, 2002), and its production and applications are increasing¹. Lactic acid, the monomer employed for PLA manufacture, can be produced by chemical or biological ways. Fermentation of sugar solutions from corn, potatoes or other feedstocks is the leading production method. Lactic acid can be converted into PLA either by gradual polycondensation or, mainly, by ring-opening of lactide, the lactic acid cyclic dimer^{3,4}.

Due to the chiral nature of lactic acid, the stereochemistry of PLA is complex. The L- and D-enantiomers of lactic acid can lead to meso or iso lactides, which can give different configurations (atactic, isotactic, heterotactic or syndiotactic) after polymerization, and with different possible block distributions, affecting both crystallinity and thermomechanical properties of the polymer^{5,6}. Commercial PLA is generally obtained from solutions containing a high proportion of L-lactic acid (~96%), via formation of lactide and further ring opening polymerization, yielding a semicrystalline material.

PLA has a thermoplastic behaviour, being suitable for melt processing, namely by injection moulding, with favourable melting point for biocomposites compounding (around 160 °C, below the temperatures at which natural fibres start to degrade)^{7,8}. PLA presents satisfactory mechanical properties, enabling its application in a variety of industrial fields, but shows a limited tenacity. Reinforcement by a suitable material is an interesting alternative for increasing stiffness and dimensional stability^{9,10}.

The interest toward natural-fibre-reinforced biodegradable polymers has considerably grown in the past few years. Compared to traditional inorganic fillers (such as glass, aramid, or carbon fibres), reinforcements of cellulosic nature are renewable, cheap, low density, and present competitive specific mechanical properties. On the other hand, cellulosic reinforcements do not affect biodegradability of the biopolymer used as a matrix^{11,12}. Recent studies have emphasized on the favourable characteristics of both natural cellulose and man-made fibres (such as Cordenka, viscose or Lyocell) as reinforcing agents for biocomposites^{10,13–16}. Natural fibre-reinforced PLA composites are finding new applications in a variety of fields, including building, packaging and manufacture of automotive components, and many commercial products of this type are currently established on the market^{17,18}.

The ability of reinforcing agents derived from lignocellulosic materials (LCM) for improving the mechanical properties of polymeric matrices de-

pends on a variety of factors, including: particle aspect ratio, fibre orientation and degree of interfacial interaction matrix-reinforcement. Poor adhesion between the two components would lead to a PLA composite of poor mechanical properties, because the stress transfer between phases would not be effective. The processing conditions used in composite manufacture affect the properties of composites, acting for example on length fibre distribution⁹, fibre orientation, and mechanical parameters¹⁹.

The aim of this study was to investigate the influence of selected parameters affecting the compounding of composites in a integrated compounding injection moulding (ICIM) process on their mechanical properties. PLA samples from different manufacturers were first characterized, and an assessment of the effects caused by the operational parameters was carried out with the best commercial compound. The interrelationships between processing parameters and composite mechanical properties were assessed using a statistical technique that enabled the development of correlations giving a quantitative interpretation of the experimental results. Surface morphology and fibre length were determined using selected probes. The results were compared with literature data obtained with a sequential extrusion-injection moulding process (SEIM).

MATERIALS AND METHODS

The composite materials considered in this work were produced from commercial PLA and waste cellulose fibres obtained from a local kraft pulp mill.

PLA

In this study, two different PLA granulates were considered: PLA-1, supplied by Natureworks, and PLA-2, supplied by Velox.

The melt flow index (MFI) was measured in a MFI CEAST at 210 °C and 21.16 N. Density (ρ) of PLA was determined according to ISO 1183-A. Determinations were carried out in triplicate.

Specific optical rotation $[\alpha]_D^{25}$ values of 10 g PLA per 1 chloroform solutions were determined at 25 °C. The D- and L-isomer contents were estimated assuming $[\alpha]_D^{25}$ values -156 and +156 for poly(L-lactic acid) and poly(D-lactic acid), respectively^{6,20}.

Cellulosic Reinforcements

The *Eucalyptus globulus* wood cellulose fibres used in this work were obtained from the wastewaters of a local kraft pulping industry (ENCE, Pontevedra, Spain). Fibres were washed and cleaned to remove extraneous material, treated with a laboratory defibrator (Ultraturrax T-50, IKA Labor-technik, Germany) and recovered by filtration. The apparent density (determined using the ASTM D1895-B method) was 0.14 kg/dm³ (the data reported correspond to the average value of triplicate assays).

Crystallinity

Crystallinity (X_c) was determined from DSC thermograms and XR diffractograms. As the crystallinity of a polymer is critically dependent on the experimental technique employed for determination, no absolute value was assigned.

Crystallinity determination by DSC. An estimate of the crystallinity of a given polymer can be made from DSC data assuming strict two-state behavior (polymer composed of distinct, non-interacting amorphous and crystalline regions)²¹. Despite the obvious limitations of this model, it is widely used in industry to assess the crystallinity of polymers. The crystallinity (X_c) is calculated using the equation

$$X_c = (\Delta H / \Delta H_{100}) \quad (1)$$

where ΔH and ΔH_{100} are the measured melting enthalpy determined for the sample and the melting enthalpy of a 100% pure crystalline sample of the same polymer, respectively. ΔH_{100} for PLA was assumed²² to be 93 J/g.

The thermal behavior of PLA samples was assessed by differential scanning calorimetry (DSC) in a TA DSC-Q20 system, using nitrogen as purge gas. Samples were heated at 10 °C/min up to 200 °C, cooled to 30 °C using liquid nitrogen, and reheated up to 200 °C at 10 °C/min. Calibrations of temperature and enthalpy scale were carried out using pure indium standard.

Crystallinity determination by X-ray diffraction (XRD). Crystallinity was calculated as the ratio between the area of peaks corresponding to ordered regions and total area in diffractograms obtained using a Bruker instrument (AXS Nanostar).

Rheological Measurements

Oscillatory shear experiments were performed in a TA ARES oscillatory rheometer, using parallel plate geometry with a plate diameter of 25 mm. PLA discs for oscillatory rheology tests were prepared by compression moulding at 170 °C, with 25 mm diameter and 1.2 mm thickness. PLA samples were dried in a vacuum oven at 50 °C overnight before utilization. Determinations were carried out in dynamic mode at 180 °C, from 0.1 to 100 Hz. The linear range of deformations was checked for all the materials assayed.

Intrinsic Viscosity Measurement

The intrinsic viscosity (η , in ml/g) measures the intrinsic volume of a polymer, and is usually used as an indicator of average molecular weight. PLA samples were dissolved in chloroform, and their intrinsic viscosity were determined from viscosity data obtained using an Ubbelohde type viscosimeter with capillaries 53001-0a (0.53 mm diameter), placed into a controlled water temperature bath at 25 °C. The concentrations of PLA in chloroform were 20.0, 10.0, 5.0 and 2.5 g/l. For every concentration, the efflux times were measured ten times. The reduced viscosity and the inherent viscosity (logarithmic viscosity number) were calculated and plotted versus concentration on the same graph. Extrapolation of the two functions at zero concentration led to the intrinsic viscosity (or limiting viscosity number).

Formulation and Testing of Composite Materials

The influence of the processing conditions on the manufacture of composite materials made up of PLA-1 (Natureworks) and cellulose fibres was assessed in selected experiments. Both PLA and fibres were vacuum dried prior to processing, according to the manufacturers instructions. The relative weight ratio cellulose fibres:PLA employed in this work was 1:4. These quantities were selected on the basis of a previous study (data not shown) and our own experience^{9,15}.

In order to establish the influence of the principal process variables on the properties of composites, the experimental plan followed an statistical (Taguchi) design, whose structure is shown in Table I. The selected factors (inputs) were: extrusion temperature (die), T_e ; injection temperature (nozzle), T_i ; mold temperature, T_m ; extrusion speed, S_e ; injection speed, S_i ; hydraulic holding pressure, P_h ; cooling time, t_c . To characterize the com-

posites, the following responses (outputs) were measured: tensile strength, σ_t ; Young modulus, E ; strain at break, ϵ . The statistical analysis enabled the development of empirical equations relating responses to the factors considered. The independent variables were normalized assigning the value -1 to the lowest limit of the variation range, and $+1$ to the highest limit. These normalized variables were denoted as the original variables with a $*$ as superscript. Table I also includes the processing conditions used in the manufacture of neat PLA probes.

ISO tensile and impact specimens were produced using an integrated compounding and injection moulding machine (twin screw extruder with a screw diameter of 35 mm, L/D ratio of 18 and injection unit with 2300 kN clamping force). The extruder feeds directly the injection zone, diminishing the mechanical and thermal stresses to which the material is submitted when compared with independent extrusion followed by injection moulding. The dimensions of ISO specimens were 80 mm length, with a constant rectangular cross-section of $10 \times 4 \text{ mm}^2$. Ten ISO tensile specimens from each experiment were tested in a Shimadzu Autograph AG-X testing machine with 50 kN load cell, at a crosshead speed of 2 mm/min. Ten impact specimens were tested in a Ceast-Resil Impactor (15 J energy) at 23°C and 55% relative humidity.

TABLE I

Taguchi's design of experiments for the factors: Extrusion temperature (die), T_e ; injection temperature (nozzle), T_i ; mould temperature, T_m ; extrusion speed, S_e ; injection speed, S_i ; hydraulic holding pressure, P_h ; cooling time, t_c

Run	T_e , °C	T_i , °C	T_m , °C	S_e , rpm	S_i , mm/s	P_h , bar	t_c , s
PLA	170	170	20	70	10	20	20
1	170	170	20	70	10	20	20
2	170	170	40	90	10	40	40
3	170	200	20	90	24	20	40
4	170	200	40	70	24	40	20
5	200	170	20	90	24	40	20
6	200	170	40	70	24	20	40
7	200	200	20	70	10	40	40
8	200	200	40	90	10	20	20

Cross and longitudinal sections of the specimens were observed by polarized light microscopy using an Olympus BH2 transmission microscope. The observed samples (10 μm thickness) were obtained using a Leitz 40 microtome, and mounted on glass lamellae.

The fibre|matrix interface morphologies were analyzed in a Leica S360 scanning electron microscope, through the observation of selected zones on fracture surfaces of moulded specimens, after being sputter coated with a thin gold layer.

With the aim to evaluate fibre damage, length distributions of cellulose fibres were measured before and after processing. Composite samples were dissolved in chloroform to 0.10 g/l concentration and observed by optical microscopy. At least 500 fibres were counted for every sample using image analyser software Leica Quantimet 500C.

RESULTS AND DISCUSSION

PLA Characterization

The values of physical, mechanical and thermal properties of the two commercial PLAs are shown in Table II. The specific optical rotation $[\alpha]_D^{25}$ obtained in both cases were close to the value of -296° corresponding to PLLA, indicating a high stereoregularity. Modulus were similar for both PLAs, with higher elongation at break (45% superior) and tensile strength (32% superior) in the case of PLA-1. The most remarkable difference is in the impact strength, with a value of 13.4 J/m for PLA-1 and 6.0 J/m for PLA-2.

The thermal properties of the two polymer matrices are manifested in the DSC data shown in Fig. 1. In the first heating (Fig. 1a), the glass transition temperature, T_g , the corresponding melting temperature, T_{melt} , and total enthalpy, ΔH , were identified or calculated (see Table II). No cold or pre-melt crystallization peaks were observed, and the total enthalpy corresponding to crystallinity of original material corresponded to the melting enthalpy. The data confirmed a different thermal behavior for PLA-1 and PLA-2. PLA-1 showed a small variation in the glass transition zone and a defined peak at the melting temperature, indicative of a high crystallinity, PLA-2 presented a clear glass transition and two distinct peaks in melting endotherms, with low enthalpy value, corresponding to a low crystallinity. The melting temperature was higher for PLA-1. Figure 1b shows the second heating trace which provided closely related results for both PLA. Only glass transition is observed, more pronounced in the case of PLA-2, with no

peak corresponding to melting, indicating that the material is amorphous. At the heating rate employed, no cold or pre-melt crystallization occurred, indicating that no reordering of polymer took place under the considered conditions. Similar behavior was observed by Lee and Lee⁷ and Martin and Avérous²³. According to Dorgan et al.⁸, this variation pattern corresponds to a linear polymer, while branched PLA undergoes a significant recrystallization along the second heating.

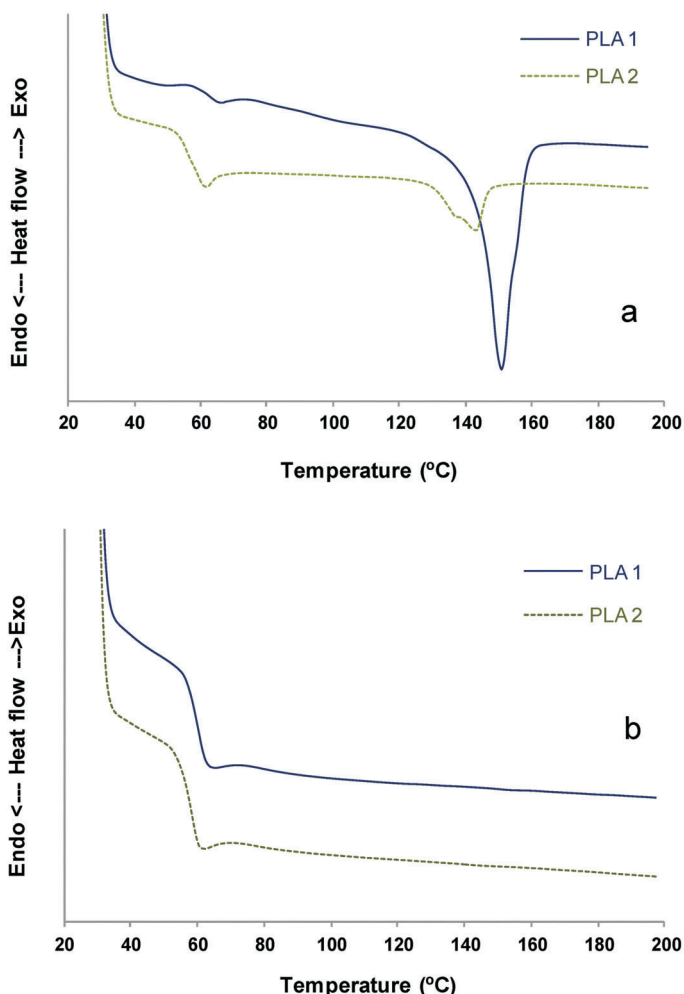


FIG. 1
DSC trace for PLA-1 (NatureWorks) and PLA-2 (Velox). First heating (a), second heating (b)

X-ray diffraction images are presented in Fig. 2. PLA-1 and PLA-2 led to different pictures, characterized by defined circles in the case of PLA-1, while the image corresponding to PLA-2 presented a more disperse diffraction. The diffractogram corresponding to PLA-1 presented clear peaks, the major one corresponding to $2\phi = 1.8$, and a minor area corresponding to

TABLE II
Properties for the polylactic acid samples evaluated

Parameter	Units	PLA-1	PLA-2
MFI	g/10 min	30.3 ± 0.5	29.6 ± 0.9
η	ml/g	148 ± 2	80 ± 2
ρ	g/cm ³	1.25 ± 0.02	1.26 ± 0.01
T_g	°C	62.5 ± 0.2	58.1 ± 1.4
T_{melt}	°C	152.1 ± 0.4	143.0 ± 0.1
ΔH	J/g	30.9 ± 0.5	6.2 ± 0.8
X_c (DSC)	%	33.6 ± 0.1	7.3 ± 0.4
X_c (XRD)	%	30.5 ± 0.5	4.1 ± 1.4
σ_t	MPa	54.7 ± 1.3	41.4 ± 1.1
E	GPa	1.5 ± 0.1	1.5 ± 0.6
ε	%	4.5 ± 0.1	3.1 ± 0.1
I_s	J/m	13.4 ± 1.6	6.0 ± 0.9

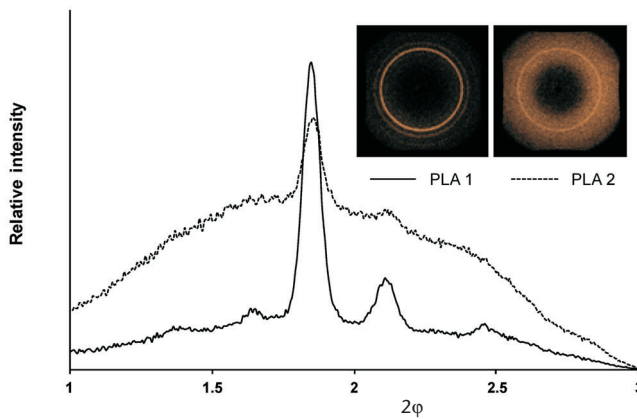


FIG. 2
X-ray diffractograms determined for PLA-1 (NatureWorks) and PLA-2 (Velox)

amorphous zone, indicating a high crystallinity. Oppositely, the PLA-2 diffractogram presented a broad area corresponding to amorphous zones. The average crystallinities determined by X-ray diffraction and DSC methods were in good agreement (see Table II).

Figure 3 shows the values of storage modulus, G' , loss modulus, G'' , and complex viscosity, η^* , obtained from oscillatory rheometry. The extrapolated values for complex viscosity at 0 rad/s were 2060 and 1179 Pa s for PLA-1 and PLA-2, respectively. In both cases, complex viscosity de-

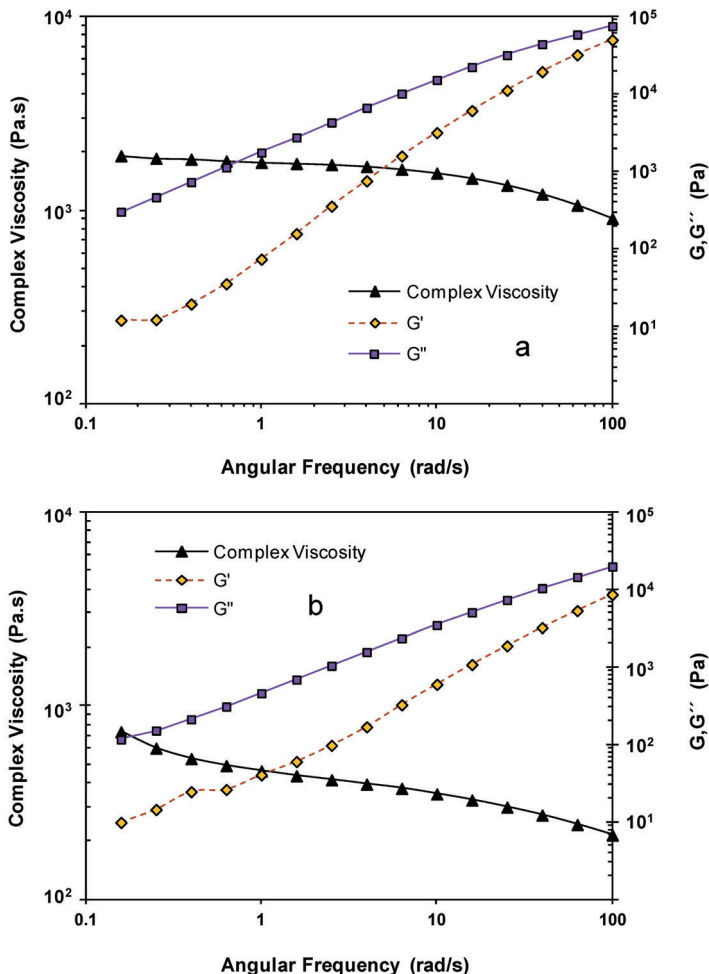


FIG. 3
Viscoelastic data determined for PLA-1 (a) and PLA-2 (b)

creased with increased angular frequency in the range of angular frequencies analyzed. PLA-1 and PLA-2 exhibited different viscoelastic behavior. PLA-1 showed minor variations up to 10 Hz, and a further decrease to reach values close to 900 Pa s at 100 Hz, while PLA-2 presented a marked drop in complex viscosity with frequency in the range analyzed, up to reach 200 Pa s at 100 Hz. In both cases G' was lower than G'' , with no cross of the curves, indicating that viscous component predominated over the elastic one.

Figure 4 presents data of reduced viscosity and inherent viscosity versus concentration. A fair linear variation can be observed for both variables in the concentration range studied, enabling the evaluation of the intrinsic viscosity by extrapolation at zero concentration. The intrinsic viscosities determined were 148.3 ml/g for PLA-1, and 80.5 ml/g for PLA-2, values

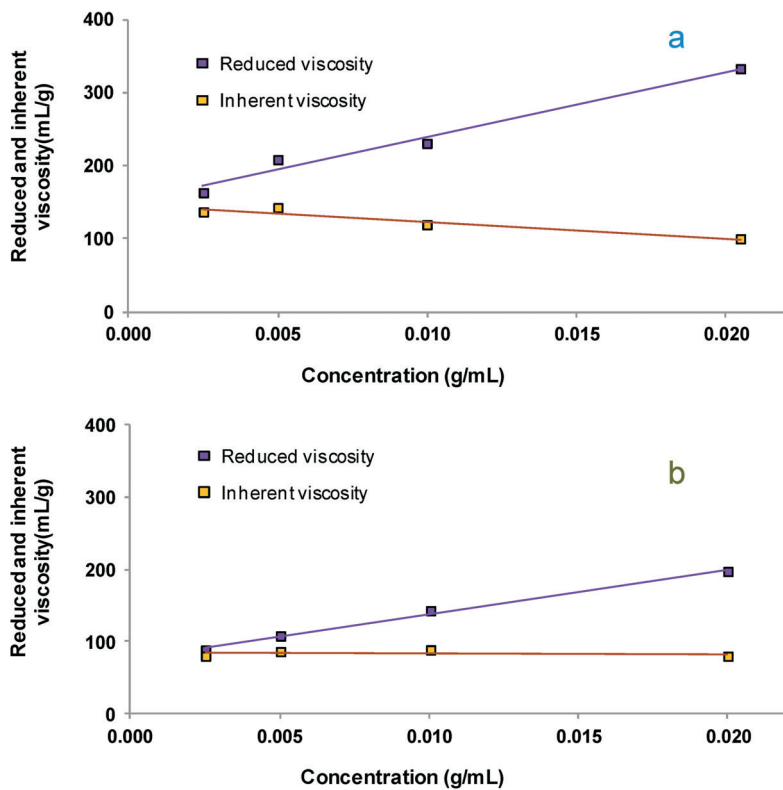


FIG. 4
Reduced viscosity and inherent viscosity versus concentration of PLA-1 (a) and PLA-2 (b)

close to that reported by other authors¹⁹. These results indicated that the average molecular weight of PLA-2 presented a lower value than that of PLA-1. According to the Mark–Houwink relationship²⁴ $[\eta] = 4.41 \times 10^{-4} M_W^{0.72}$ ($[\eta]$ in dl/g), the calculated values of M_W are 7.9×10^4 and 3.4×10^4 g/mol for PLA-1 and PLA-2, respectively.

Manufacture and Properties of Composites

According to literature, the E modulus of cellulose-filled composites is expected to increase significantly with respect to the one of the neat matrix, whereas the tensile strength should remain unaffected, and the elongation is expected to be reduced significantly²⁵. Figure 5 shows the values of mechanical properties for PLA and composites made of cellulose fibres and PLA compounded at a cellulose fibres:PLA mass ratio of 1:4. PLA probes were obtained under the conditions of experiment 1 (Table I).

All the conditions assayed led to satisfactory results in terms of stiffness. Composites presented higher values of E modulus than the non-reinforced sample, with a variation range of 2.08–2.28 GPa (corresponding to 40–53% increase respect the values determined for neat PLA probes, respectively). As the values of the processing factors were normalized before calculations, their relative importance is measured by the absolute values of the coefficients obtained when fitting the experimental data to Eq. (2).

$$E = 2.23 + 0.036 T^*_e + 0.024 T^*_i - 0.0063 S^*_i - 0.041 T^*_m + \\ + 0.0038 P^*_h - 0.024 t^*_c - 0.039 S^*_e \quad (2)$$

According to the above idea, it can be concluded that the most influential operational parameters were the mould temperature (T_m), extrusion speed (S_e) and extrusion temperature (T_e), showing a minor influence the injection temperature (T_i) and the cooling time (t_c). All factors have little influence on E , being positive (increment of response when the factor increases) for T_e , T_i and P_h , and negative for S_i , T_m , t_c and S_e .

The situation was very different when considering the mechanical strength, which presented a variation close to 140%. The maximum and minimum values of tensile stress were 56.6 and 23.6 MPa, with an increase of 3.5% and a decrease of 57%, respectively, respect to the values determined for neat PLA probes. The influence of the considered factors on the mechanical strength is described by the following equation

$$\sigma_t = 40.71 - 6.98T^*_e - 7.41T^*_i + 0.19S^*_i - 2.85T^*_m + \\ + 5.57P^*_h - 5.1t^*_c + 0.72S^*_e \quad (3)$$

which showed that the most influential processing factors were T_e , T_i and t_c (all of them with negative influence), and P_h (with positive influence). In order to allow an easier interpretation of results, Fig. 6 shows the predicted dependence of the tensile strength on T_i and T_e .

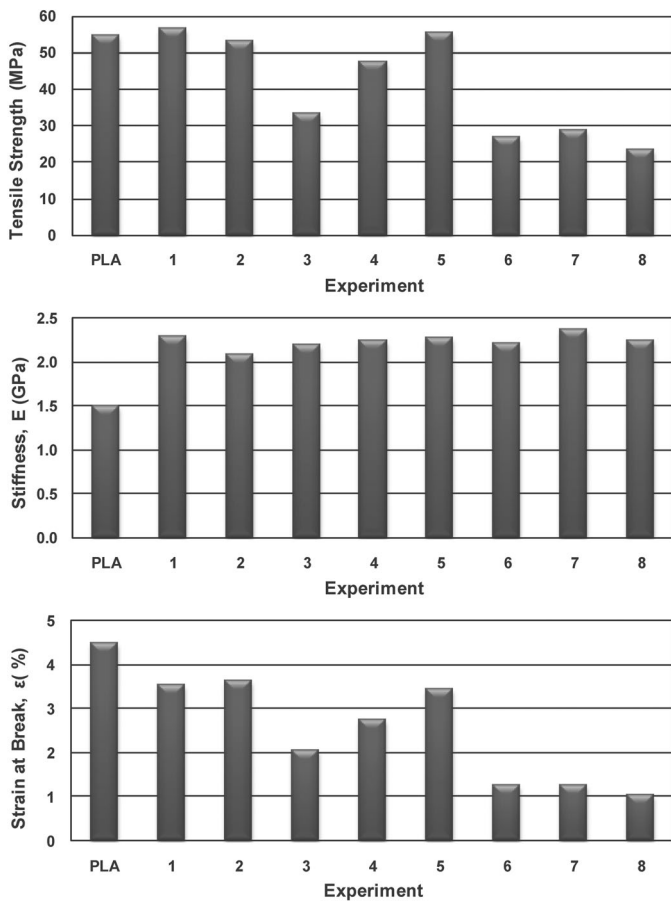


FIG. 5

Results obtained in tensile tests for neat PLA probes and composites obtained under the conditions of experiments 1 to 8 in Table I

Reinforcement resulted in increased brittleness and in shorter elongation (4.49% as an average) respect to virgin PLA probes. These latter presented a variation range for the strain at break of 3.61–1.04% (percentage of variation, 247%). The experimental data were fitted to yield the following equation

$$\begin{aligned} \varepsilon = & 2.36 - 0.614T^*_e - 0.593T^*_i + 0.0063S^*_i - 0.20T^*_m + \\ & + 0.40P^*_h - 0.32t^*_c + 0.17S^*_e \end{aligned} \quad (4)$$

which confirm that the most influential factors were the same as of the ones discussed for tensile strength, which also affected in the same sense. Figure 5 confirms the close relation between the variation patterns predicted for tensile strength and elongation. Taking into account that stiffness presented a narrow variation range, it can be seen that the tensile strength was fairly proportional to the elongation achieved by the probe in the moment of fracture.

According to literature, fibre-based composites usually present decreased impact strengths respect to the matrix, due to the poor interaction between the fibres and the matrix. Figure 7 shows the data determined for the impact tests (I_s). Interestingly, it can be observed that all composites except that obtained under the conditions of experiments 6, 7 and 8 presented

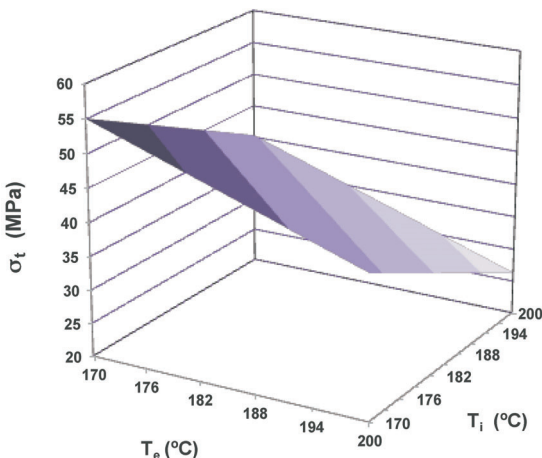


FIG. 6

Calculated dependence of the tensile strength (σ_t) on the injection temperature (T_i) and extrusion temperature (T_e)

higher impact strengths than virgin PLA, indicating effective reinforcement of the material.

Dispersion of fillers in the matrix was assessed by optical microscopy of longitudinal and transversal probe cuts. Figure 8 presents optical microscopy images of probes obtained under the conditions of experiments 1 and

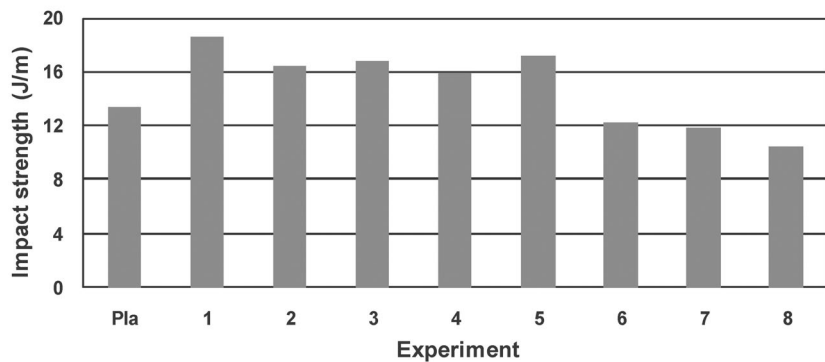


FIG. 7

Results of impact test determined for neat PLA probes and composites obtained under the conditions of experiments 1 to 8 in Table I

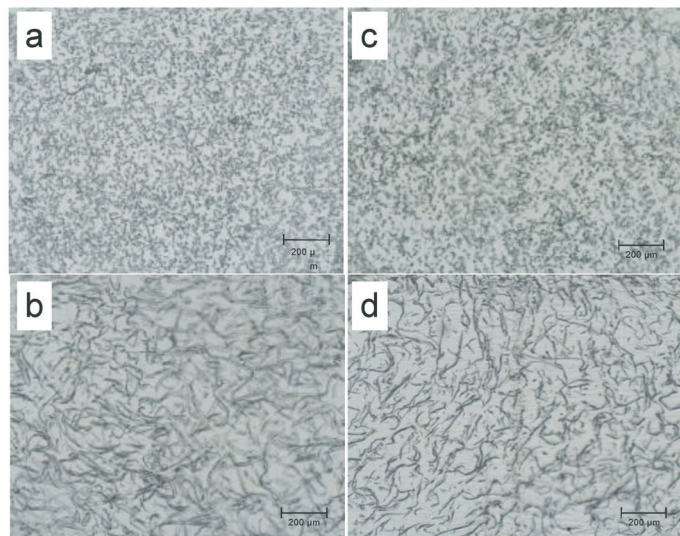


FIG. 8

Optical images of transversal cut, exp. 1 (a); longitudinal cut, exp 1 (b); transversal cut, exp. 8 (c); longitudinal cut, exp. 8 (d) (see Table I for experimental conditions)

8, which corresponded to the mildest and severest conditions, respectively. The pictures confirm a good dispersion of reinforcements in all cases, with no clear orientation. Figure 9 shows images of fibre length distributions (measured for composites manufactured under the conditions of experiments 1 and 8) at two different stages, before and after processing. Before processing, cellulose fibres presented an average length of 0.846 mm. After processing, fibres in probes obtained under the mild conditions of experiment 1 presented an average length of 0.813 mm (showing scarce degradation and no fibre breakage). Even under the severe conditions of experiment 8, the average fibre length decreased only to 0.557 mm (34.2% respect to the original fibre). Conventional sequential extrusion and injection moulding techniques lead to much higher levels of fibre breakage⁹.

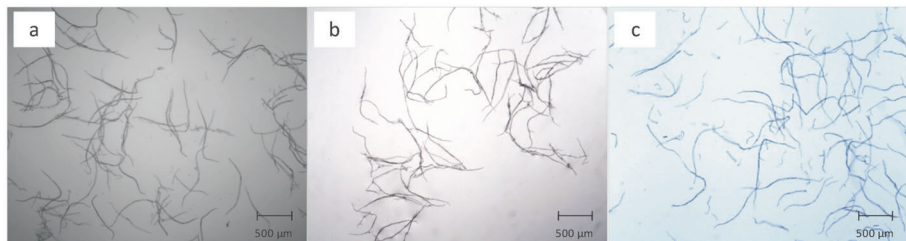


FIG. 9

Optical images of fibre length distribution: before processing (a); after processing, exp. 1 (b); after processing, exp. 8 (c) (see Table I for experimental conditions)

TABLE III

Variation (%) in mechanical properties of manufactured cellulose-PLA composites respect to virgin PLA, and in the aspect ratio (L/D) of the fibres in composites respect to original fibres, for sequential extrusion-injection moulding (SEIM) and integrated compounding-injection moulding (ICIM) techniques

Parameter	Variation, %	
	SEIM	ICIM
σ_t	-5.44	3.45
E	57.5	53.0
ε	-40.3	-21.8
I_s	-22.7	38.7
L/D	-86.3	-3.90

Figure 10 show SEM images of the surfaces of selected probes obtained under conditions 1 and 8 coming from the tensile fracture test. The images are in good agreement with the mechanical properties determined for the produced composites. Images corresponding to experiment 8 show smaller and more degraded fibres than in the case of experiment 1.

Table III shows a comparison of the results obtained in this work (using an ICIM) with the ones obtained with conventional processing (sequential extrusion and injection moulding machine, SEIM)⁹. Table III includes the

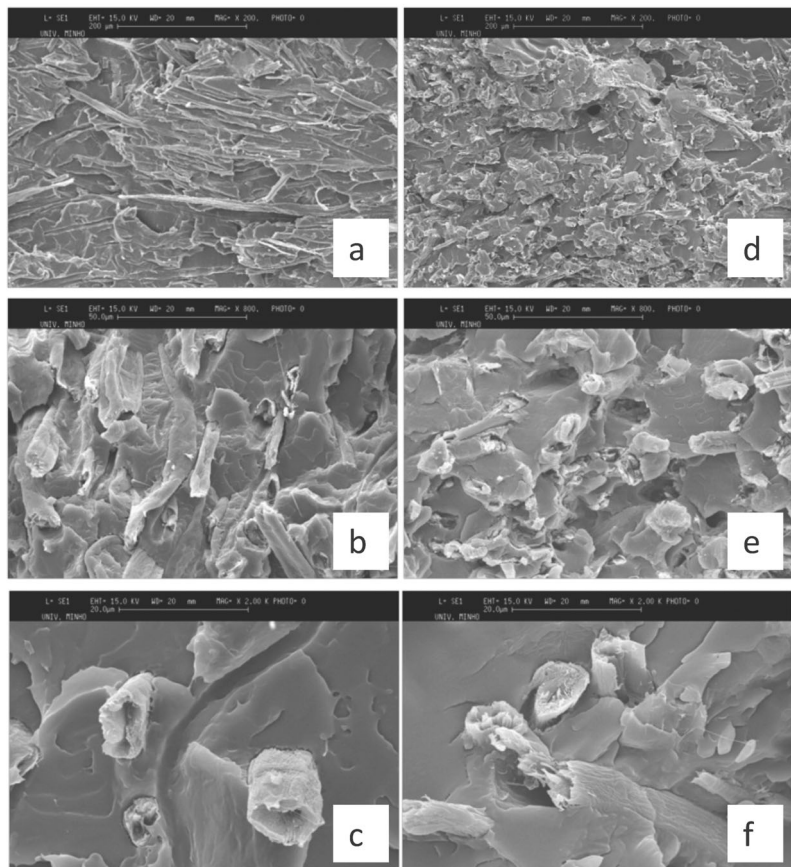


FIG. 10

SEM images of tensile fracture surfaces: exp. 1 ($\times 200$) (a), exp. 1 ($\times 800$) (b), exp 1 ($\times 2000$) (c), exp. 8 ($\times 200$) (d), exp. 8 ($\times 800$) (e), exp. 8 ($\times 2000$) (f) (see Table I for experimental conditions)

percentages of variation of the mechanical properties of the composites respect to the data determined for neat PLA probes, as well as the results concerning the aspect ratio (length/diameter) of the cellulose fibres in the original fibres and in the composites. The results show that composites manufactured with an ICIM exhibited significantly better mechanical properties than those produced by conventional SEIM, with lower fibre degradation. Interestingly, the composites produced with ICIM presented increased impact strengths respect to neat PLA probes, whereas the opposite situation was observed for SIEM-processed samples. The use of processing conditions with lower temperatures (in extrusion and moulding) also leads to better results which should be associated to lower thermal degradation of the polymer matrix.

CONCLUSIONS

This study provides an assessment on the effects of the processing conditions on the mechanical properties of PLA-cellulose composites samples produced with an integrated compounding-injection moulding machine (ICIM). In order to measure the influence of the major processing parameters on the composites mechanical properties, a set of experiments based in a statistical Taguchi's design was considered. Empirical equations describing the influence of the considered operational parameters on the composites mechanical properties were derived. The most influential operating parameters were the temperatures used in injection (T_i) and in extrusion (T_e) which caused adverse effects (higher temperatures led to inferior mechanical properties). The variables defining the injection moulding conditions (hydraulic holding pressure (P_h) and cooling time (t_c)) were also influential. Combinations of high hydraulic holding pressure and a short cooling time resulted in improved mechanical properties. The effect of the selected operational variables were particularly important in the cases of tensile strength and strain at break (which presented related variation patterns), and impact strength. Comparatively, stiffness was less affected. A comparison of the experimental data with literature information confirmed that the integrated compounding and injection moulding (ICIM) technology provided composites with better mechanical properties and lower fibre degradation than the conventional sequential extrusion and injection moulding (SEIM) technology.

The authors are in debt to Prof. A. Covas (IPC – Institute for Polymers and Composites, Department of Polymer Engineering, University of Minho, Campus de Azurém, 4800-058 Guimarães,

Portugal) for the support given during the design of the integrated compounding and injection moulding machine.

REFERENCES

1. Shen L., Worrell E., Patel M.: *Biofuels Bioprod. Bioref.* **2010**, 4, 25.
2. Queiroz A. U. B., Collares-Queiroz F. P.: *Polym. Rev.* **2009**, 49, 65.
3. Albertsson A.-C., Varma I. K.: *Adv. Polym. Sci.* **2002**, 157, 1.
4. Okada M.: *Prog. Polym. Sci.* **2002**, 27, 87.
5. Kakuta M., Hirata M., Kimura Y.: *Polym. Rev.* **2009**, 49, 107.
6. Chabot F., Vert M., Chapelle S., Granger P.: *Polymer* **1983**, 24, 53.
7. Lee S., Lee J. W.: *Korea-Australia Rheol. J.* **2005**, 17, 71.
8. Dorgan J. R., Lehermeier H., Mang M.: *J. Polym. Environ.* **2000**, 8, 1.
9. Cunha A. M., Campos A. R., Cristovao C., Vila C., Santos V., Parajó J. C.: *Plast. Rubber Compos.* **2006**, 35, 233.
10. Mathew A. P., Oksman K., Sain M.: *J. Appl. Polym. Sci.* **2005**, 97, 2214.
11. Jacob M., Thomas S.: *Carbohydr. Polym.* **2008**, 71, 343.
12. Wibowo A. C., Mohanty A. K., Misra M., Drzal L. T.: *Ind. Eng. Chem. Res.* **2004**, 43, 4883.
13. Bax B., Müssig J.: *Compos. Sci. Technol.* **2008**, 68, 1601.
14. Ganster J., Fink H. P.: *Cellulose* **2006**, 13, 271.
15. Vila C., Campos A. R., Cristovao C., Cunha A. M., Santos V., Parajó J. C.: *Compos. Sci. Technol.* **2008**, 68, 944.
16. Huda M. S., Mohanty A. K., Drzal L. T., Schut E., Misra M.: *J. Mater. Sci.* **2005**, 40, 4221.
17. Ashori A.: *Bioresour. Technol.* **2008**, 99, 4661.
18. Graupner N., Herrmann A. S., Müssig J.: *Compos. Part A* **2009**, 40, 810.
19. Ghosh S., Viana J. C., Reis R. L., Mano J. F.: *Polym. Eng. Sci.* **2007**, 47, 1141.
20. Sarasua J. R., Prud'homme R. E., Wisniewski M., Le Borgne A., Spassky N.: *Macromolecules* **1998**, 31, 3895.
21. Hatakeyama T., Quinn F. X.: *Thermal Analysis. Fundamentals and Applications to Polymer Science*. John Wiley and Sons, New York 1994.
22. Fischer E. W., Sterzel H. J., Wegner G.: *Kolloid-Z. u. Z Polymere* **1973**, 251, 980.
23. Martin O., Avérous L.: *Polymer* **2001**, 42, 6209.
24. Garlotta D.: *J. Polym. Environ.* **2001**, 9, 63.
25. Georgopoulos S. T., Tarantili P. A., Avgerinos E., Andreopoulos A. G., Koukios E. G.: *Polym. Degrad. Stab.* **2005**, 90, 303.